Change of Molecular Aggregation State in Amorphous Region with Uniaxial Extension of Preoriented Polypropylene

K. YAMADA and M. TAKAYANAGI, *Department of Applied Chemistry, Faculty of Engineering, Kyushu University, Fukuoka 812, Japan*

Synopsis

Preoriented isotactic polypropylene was uniaxially drawn at various testing directions and testing temperatures. Change of the molecular aggregation state in amorphous region with extension was elucidated by measurements of melting temperature, enthalpy of fusion, and birefringence at each stage of extension. Melting temperature depends on both crystallite thickness and orientation function of amorphous chains. It is assumed that the enthalpy change of amorphous region takes place when oriented amorphous chains are transformed into random state by heating. The ratio of the enthalpy change of amorphous region in the sample after extension to that in the sample before extension monotonously increased with increasing orientation function of amorphous chains, f_a, independent of testing direction and testing temperature. Increase of true stress with drawing led to increase of f_a. Increase of f_a with extension depended on the testing angle θ between the testing direction and the direction of the crystal c-axis of the preoriented sample, and f_a most remarkably increased in extension at $\theta = 45°$.

INTRODUCTION

Meinel and Peterlin[1] studied the change of crystallinity, elastic modulus, and tensile strength of drawn samples with various draw ratios together with the true stress–strain curves of bulk-crystallized polyethylene to establish correlations with morphological changes occurring during plastic deformation. Changes of crystallinity at draw ratios below 5 were explained by the formation of microfibrils with crystallinity independent of the thermal history of the film which depends only upon the drawing temperature. The microfibrils slide past each other at higher draw ratios, generating an increasing number of intermicrofibrillar tie molecules, which are reflected in the increase of crystallinity, elastic modulus, and tensile strength.

Arridge and Barham[2] stated that the load-elongation behavior at the post-neck-drawing stage in the deformation of crystalline polymers is modelled quantitatively by an aligned short-fiber composite in which crystalline fibrils form the reinforcing phase in a matrix of less well-ordered material. Three modes of deformation are shown to correspond to the observed load-elongation relations in polyethylene and polypropylene. The modes are (1) elastic-plastic crystals in an elastic matrix, (2) elastic-plastic crystals in an elastic-plastic matrix, and (3) elastic crystals in an elastic-plastic matrix.

Melting experiments of undrawn and drawn polyethylene performed by Peterlin and Meinel[3] show a linear increase of melting point and a reduction of heat content of the noncrystalline component with increasing draw ratio. According to Peterlin and Meinel,[3] the tied macromolecules partly incorporated

CCC 0021-8995/82/093479–13$02.30

in more than one crystal are under high strain, as consequence of plastic deformation during drawing. Harland et al.[4] demonstrated that the melting behavior of the drawn fibers of polyethylene was accounted for in terms of the rupture of a fraction of the original lamellar structure and the growth of a new crystalline structure. The melting behavior of restrained isotactic polypropylene fibers was examined quantitatively by Samuels.[5] Noncrystalline chain orientation influences the endotherm temperature through its changing configurational entropy and the noncrystalline chain must be considered as plastically deformed, since rubber elasticity theory is not followed as predicted.[5]

In our previous work,[6,7] the strain on uniaxial extension of preoriented isotactic polypropylene, which was prepared by extruding through T-die from molten state, was separated over the whole range of deformation into three processes: (1) crystallite boundary slip (A_1 process), (2) uniform shear deformation of crystallite (A_2 process), and (3) restoration of molecular orientation from the shear-deformed state ($\overline{A_2}$ process). The preoriented polypropylene having a relatively simple superstructure was conveniently used to elucidate various mechanisms of deformation accompanied by the superstructural changes. Both the A_1 and A_2 processes predominate before the $A_2 \rightarrow \overline{A_2}$ transition takes place at the critical value of true strain. After the $A_2 \rightarrow \overline{A_2}$ transition takes place, the specimen may be deformed by a molecular process such as pulling out or scission of the isolated extended chains from the folded chain crystals being followed by their refolding.

In this work, change of molecular aggregation state in amorphous region during uniaxial extension of preoriented isotactic polypropylene is investigated by measuring melting temperature, heat of fusion, and orientation function of amorphous chain. The deformations associated with crystallities in extension were mainly examined in the previous work.[6,7] The relationship between strain hardening and change of amorphous structure during extension is obtained by stretching the preoriented specimen at various testing temperatures and various testing directions to its molecular axis, and how the change of amorphous structure is related to the increase of true stress in extension is elucidated.

EXPERIMENTAL

Specimen

A T-die sheet of isotactic polypropylene (Noblen, MFR = 2.8) used as preoriented crystalline polymer was prepared by means of T-die extrusion under the conditions that the temperature of the top of T-die was 543 K, the winding temperature 415 K, the winding speed 15 mm/min, and the draw ratio about 5.2. Specimen used for uniaxial extension was cut out of the T-die sheet in such a way that the angles θ between testing direction and crystal c-axis of the T-die sheet are 0°, 45°, and 90°. The width and thickness of the specimen were 5 mm and 0.3 mm, respectively.

Uniaxial Extension

The preoriented specimen was uniaxially extended at testing temperatures of 313 K, 373 K, and 403 K with a tensile tester, Tensilon UTM-3 (Toyo Baldwin Co., Ltd.). Testing speed was 5 mm/min and gage length 20 mm.

DSC Measurement

Melting behavior of the specimens obtained with uniaxial extension of preoriented specimen was measured with differential scanning calorimeter (DSC), Unix (Rigaku Denki Co., Ltd). Weight of sample measured was 0.4 mg and heating rate 5 K/min.

Density

Density was measured at 298 K by means of a floating method using ethanol–water mixture.

X-Ray Measurement

Long periods were calculated on the basis of Bragg's law, using the distance between the meridional spots of maximum intensity of small-angle X-ray scattering (SAXS) photograph obtained by an X-ray generator, Rotaunit RU-3 (Rigaku Denki Co., Ltd.). The orientation function of the crystal c-axis was evaluated from the (110) and (040) planes azimuthal intensity distributions of X-ray diffraction by the usual method.[8]

Birefringence

Birefringence was measured at room temperature with a polarization microscope, POH (Nippon Kogaku Co., Ltd.).

RESULTS AND DISCUSSION

Variation of Melting Temperature with Uniaxial Extension

Figures 1(a) and (b) show the variations of melting temperature as a function
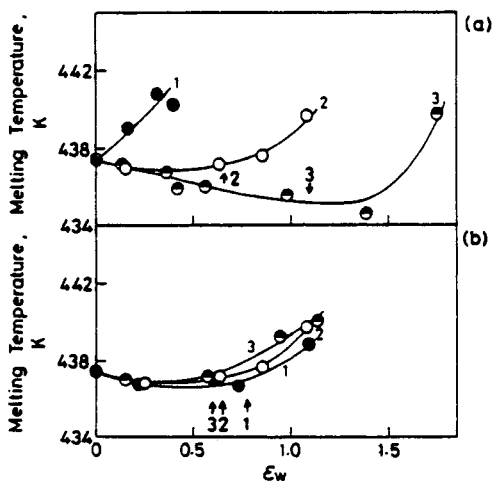

Fig. 1. Melting temperature vs. ϵ_W in extension (a) at $\theta = 0°$ (●), 45° (○), and 90° (◉) and $T_t = 373$ K and (b) at $\theta = 45°$ and $T_t = 313$ K (●), 373 K (○), and 403 K (◉). The arrows in the figure indicate the regions, in which the $A_2 \rightarrow \overline{A}_2$ transition takes place.

of the natural logarithm of the ratio of width reduction ϵ_W, (a) at testing directions θ of 0°, 45°, and 90° and testing temperature T_t of 373 K, and (b) at θ = 45° and T_t = 313 K, 373 K, and 403 K, respectively. The ϵ_W is evaluated by the following equation:

$$\epsilon_W = \ln(W_0/W)$$

where W_0 and W are the widths of the specimen before and after stretching, respectively. At θ = 45° or 90°, the width reduction of the specimen is much larger than the thickness reduction,[6] and therefore the value of ϵ_W is assumed to be nearly equal to the true strain ϵ. At θ = 0°, the decrease of width is nearly equal to that of thickness and therefore $\epsilon \simeq 2\epsilon_W$. The temperature of main endothermic peak was adopted as the melting temperature. Under all the testing conditions except for θ = 0° and T_t = 373 K, the melting temperature first decreased with uniaxial extension, then increased, and finally became higher than that of the original T-die sheet. The regions of the $A_2 \rightarrow \overline{A_2}$ transition are indicated by the arrows in the figure, in which the values of ϵ_W are 0.66 for θ = 45° at T_t = 373 K, 1.1 for θ = 90° at T_t = 373 K, 0.78 for θ = 45° at T_t = 313 K, and 0.60 for θ = 45° and T_t = 403 K.[7] At θ = 0°, the A_2 process does not take place and therefore the $A_2 \rightarrow \overline{A_2}$ transition could not be found out. The $A_2 \rightarrow \overline{A_2}$ transition region almost corresponds to the transition region of the melting temperature from decreasing to increasing with ϵ_W under each testing conditions. At θ = 0° and T_t = 373 K the melting temperature monotonously increased with extension.

The melting temperature $T_m(l_c)$, of lamellar crystals with finite thickness, l_c, is always lower than the melting temperature T_m° of perfect crystals in which the effect of surface energy can be neglected. According to Hoffman and Weeks[9] and Hirai and Yamashita,[10] melting temperature of lamellar crystals with thickness of l_c is represented by the following equation:

$$T_m(l_c) = T_m^\circ \left(1 - \frac{2\sigma_e}{\Delta h_f l_c}\right) \tag{1}$$

where Δh_f is the enthalpy of fusion of lamellar crystals per unit volume and σ_e the free energy of lamellar surface including folded chains. According to Fatou,[11,12] the values of T_m°, Δh_f, and σ_e for isotactic polypropylene are 481 K, 5.80 kJ/mol, and 28.5 μJ/cm^2, respectively.

The melting temperature of a mat of single crystals depends on a long period[13] evaluated by using SAXS photograph. The long period is assumed to correspond to the thickness of single crystal, l_c, in a crystal mat. However, a significant weight fraction of amorphous region is contained in the polypropylene (PP) specimen used in this work, and it may be said that the melting temperature of PP depends on the thickness of crystallites rather than the long period. The thickness of crystallites, l_c, can be evaluated by the following equation:

$$l_c = L(\rho - \rho_a)/(\rho_c - \rho_a) \tag{2}$$

where L is long period, ρ_c the density of crystalline region, ρ_a the density of amorphous region, and ρ the density of sample. According to Danusso et al.,[14] the values of ρ_c and ρ_a are 0.935 g/cm^3 and 0.857 g/cm^3 at 298 K, respectively. Figures 2(a) and (b) show the variation of crystallite thickness with uniaxial extension (a) at θ = 0°, 45°, and 90° and T_t = 373 K and (b) at θ = 45° and T_t

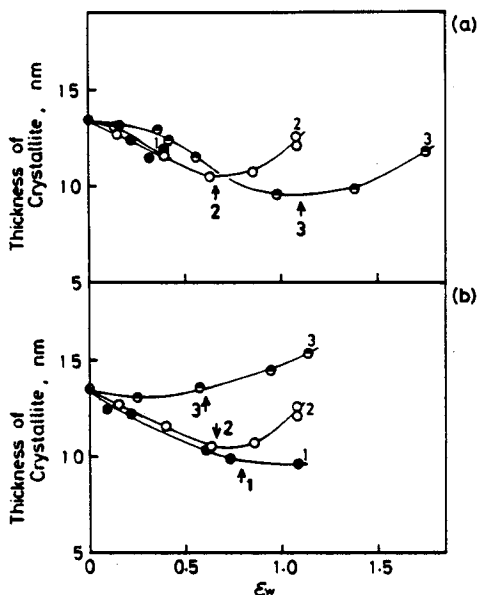Fig. 2. Thickness of crystallite vs. ϵ_W in extension (a) at $\theta = 0°$ (●), 45° (○), and 90° (◓) and T_t = 373 K and (b) at $\theta = 45°$ and T_t = 313 K (●), 373 K (○), and 403 K (◓).

= 313 K, 373 K, and 403 K, respectively. The crystallite thickness l_c was evaluated by using eq. (2) and the measured values of L and ρ. In all the testing conditions, l_c decreased with extension in the earlier stage of extension (namely, before the $A_2 \rightarrow \overline{A_2}$ transition took place at $\theta = 45°$ or 90°). However, l_c increased in the later stage of extension (namely, after the $A_2 \rightarrow \overline{A_2}$ transition took place at $\theta = 45°$ or 90°) in three testing conditions, that is, at $\theta = 45°$ and T_t = 373 K, at $\theta = 45°$ and T_t = 403 K, and at $\theta = 90°$ and T_t = 373 K. On the other hand, l_c did not increase in the other testing conditions, that is, at $\theta = 0°$ and 373 K and at $\theta = 45°$ and T_t = 313 K. It became apparent from the behavior of l_c in Figure 2 that the crystallite thickness depended on the testing temperature after the $A_2 \rightarrow \overline{A_2}$ transition took place at $\theta = 45°$ or 90°. In the previous work,[6] this fact was explained by the molecular process of plastic deformation in which extended chains are refolded to form crystallites with the new thickness depending on the testing temperature T_t after they are pulled out of the crystallites by overcoming the intermolecular force to restrain them in the crystallites. Such a molecular process initiates after the $A_2 \rightarrow \overline{A_2}$ transition takes place at $\theta = 45°$ or 90°, but does from the beginning of extension at $\theta = 0°$.[6,7]

According to the previous work,[6,7] the T-die sheet possesses the superstructure in which lamellar crystals composed of crystallites are also the structural elements of the microfibrils which orient parallel to the machine direction. When the oriented specimen with the above superstructure was uniaxially extended in such a way that the angle between the testing direction and the molecular axis was 45° or 90°, the crystallite thickness was decreased in the earlier stage of extension by the uniform shear deformation of crystallites.[6,7] Therefore, the melting temperature of the crystallites, $T_m(l_c)$, should be decreased in the earlier stage of extension at $\theta = 45°$ or 90°, so long as eq. (1) is valid. This explanation is supported by the results of Figure 1.

In the later stage of extension at $\theta = 45°$ or 90°, the crystallite thickness was

increased with extension in all the testing conditions except for $\theta = 45°$ and T_t = 313 K, but the value of l_c in the final stage of extension became always smaller than that before extension in all the testing conditions except for $\theta = 45°$ and $T_t = 403$ K. This fact shows that in all the testing conditions except at $\theta = 45°$ and $T_t = 403$ K, the melting temperature should be always lower than that of the original T-die sheet. However the melting temperature actually measured in the final stage of extension always became higher than that before extension, as shown in Figure 1. This fact suggests that the melting temperature is not affected only by the crystallite thickness, but the other factor affecting the melting temperature must be taken into consideration. According to Samuels,[5] the melting temperature of oriented isotactic polypropylene increases with increasing orientation function of amorphous chains. On the basis of the Samuels' idea, it can be presumed that the melting temperature in the later stage of extension at $\theta = 45°$ or $90°$ is not only affected by crystallites thickness but also by orientation function of amorphous chains. At $\theta = 0°$ and $T_t = 373$ K, the melting temperature is evidently affected by orientation function of amorphous chains, since the crystallite thickness monotonously decreased with extension but the melting temperature increased. Orientation function of amorphous chains will be evaluated in the later section, and the effect of orientation function of amorphous chains on the melting temperature will be ascertained.

Variation of "Melting" Enthalpy of Amorphous Region with Uniaxial Extension

It is assumed that the enthalpy change of amorphous region takes place when oriented amorphous chains are transformed into random state by heating. Such an enthalpy change is hereafter termed "melting" enthalpy of amorphous region. The melting enthalpy of sample, ΔH_f, can be evaluated from measuring the melting peak area on DSC curve. It should be noted that the peak area also depends on both weight of sample and heating rate.[15,16] In this work, the sample weight of 0.4 mg and the heating rate of 5 K/min were adopted. According to Peterlin and Meinel,[3] the melting enthalpy of a sample of semicrystalline polymer, ΔH_f, can be represented by the following equation:

$$\Delta H_f = H_l - H_s = H_l - [\alpha_m(H_c + 2\sigma_e/L) + (1 - \alpha_m)H_{as}] \qquad (3)$$

where H_l is enthalpy in a molten state, H_s enthalpy of the sample, H_c enthalpy of the crystalline part, H_{as} enthalpy of the amorphous part, α_m weight fraction of crystalline part, σ_e surface-free energy of crystallite, and L the long period. Since it is more appropriate to use crystallite thickness l_c, as shown in Figure 2, rather than long period L in eq. (3), eq. (3) should be corrected to the following equation:

$$\Delta H_f = H_l - [\alpha_m(H_c + 2\sigma_e/l_c) + (1 - \alpha_m)H_{as}] \qquad (4)$$

The "melting" enthalpy of the amorphous region, $(H_l - H_{as})$, is obtained from eq. (4) as follows:

$$H_l - H_{as} = \frac{\Delta H_f}{1 - \alpha_m} - \frac{\alpha_m}{1 - \alpha_m}\left[(H_l - H_c) - \frac{2\sigma_e}{l_c}\right] \qquad (5)$$

where the value of $(H_l - H_c) = \Delta h_f$, the heat of fusion of pure crystal, is 5.80

kJ/mol[11,12] and the value of σ_e is 28.5 μJ/cm^2.[11,12]   The value of α_m is obtained by use of measured density of the specimen, ρ, and both the densities of the crystalline region, ρ_c, and the amorphous region, ρ_a, given by Danusso et al.,[14] with the following equation:

$$\alpha_m = \frac{\rho_c}{\rho} \frac{\rho - \rho_a}{\rho_c - \rho_a} \qquad (6)$$

Figures 3(a) and (b) show the variation of measured melting enthalpy of the semicrystalline PP, ΔH_f, with uniaxial extension (a) at $\theta = 0°, 45°$, and $90°$ and $T_t = 373$ K, and (b) at $\theta = 45°$ and $T_t = 313$ K, 373 K, and 403 K, respectively. The relationship between ΔH_f and ϵ_W is similar to the relationship between T_m and ϵ_W, as shown in Figure 1.   The value of ΔH_f increased in the later stage of extension under all the testing conditions after taking the minimum point in some cases.   Figures 4(a) and (b) show the ratio of "melting" enthalpy of amorphous region after extension, $(H_l - H_{as})$, to that before extension, $(H_l - H_{as})_0$, $(H_l -$
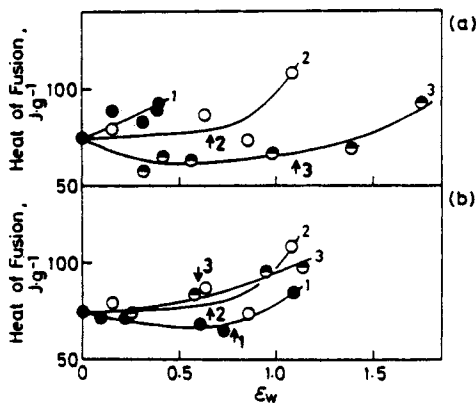

Fig. 3. Measured heat of fusion vs. ϵ_W in extension (a) at $\theta = 0°$ (●), 45° (○), and 90° (◒) and T_t = 373 K and (b) at $\theta = 45°$ and T_t = 313 K (●), 373 K (○), and 403 K (◒).
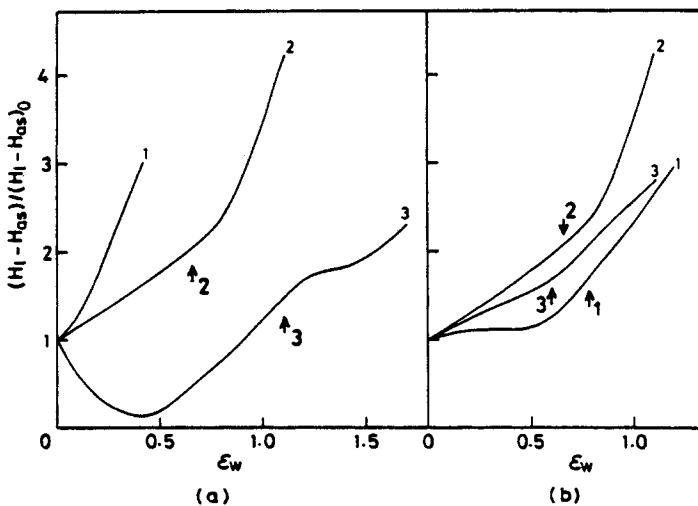

Fig. 4. $(H_l - H_{as})/(H_l - H_{as})_0$ evaluated by eq. (5) vs. ϵ_W in extention (a) at $\theta = 0°$ (1), 45° (2), and 90° (3) and T_t = 373 K and (b) at $\theta = 45°$ and T_t = 313 K (1), 373 K (2), and 403 K (3).

$H_{as})/(H_l - H_{as})_0$, as a function of ϵ_W (a) at $\theta = 0°, 45°$, and $90°$ and $T_t = 373$ K and (b) at $\theta = 45°$ and $T_t = 313$ K, 373 K, and 403 K, respectively. The values of $(H_l - H_{as})_0$ and $(H_l - H_{as})$ were evaluated by using eq. (5) and the values of ΔH_f given in Figure 3. In all the testing conditions except for $\theta = 90°$ and $T_t = 373$ K, the value of $(H_l - H_{as})_0$ increased with extension and did so more remarkably in the later stage of extension. At $\theta = 90°$ and $T_t = 373$ K, the value of $(H_l - H_{as})/(H_l - H_{as})_0$ temporarily decreased with extension and then increased. The remarkable increase of $(H_l - H_{as})/(H_l - H_{as})_0$ in the later stage of extension for $\theta = 45°$ and $90°$ almost initiated after the $A_2 \rightarrow \overline{A_2}$ transition, the regions of which are indicated by the arrows in Figure 4.

If amorphous chains are oriented along molecular axis of crystallites by extension, the intramolecular energy of amorphous region may decrease. Also if the amorphous chains are closely packed by the above orienting,[3] intermolecular energy may decrease. The enthalpy of amorphous region, H_{as}, is equal to the sum of the intramolecular and intermolecular energies.[3] Since H_l is a constant, the value of $(H_l - H_{as})$ should be increased, if the orientation function of amorphous chains is increased by extension. The orientation function of amorphous chains will be evaluated in the following section.

Variation of Orientation Function of Crystal C-Axis and Orientation Function of Amorphous Chains with Uniaxial Extension

Figures 5(a) and (b) show the variation of orientation function of the crystal c-axis, f_c, with extension (a) at $\theta = 0°, 45°$, and $90°$ and $T_t = 373$ K and (b) at $\theta = 45°$ and $T_t = 313$ K, 373 K, and 403 K, respectively. The orientation function of the crystal c-axis, f_c, does not refer to the degree of orientation of the crystal c-axis along the stretching direction, but to that along the orienting direction in the stretched sample. The orienting direction in the stretched sample corresponds to the direction along which a major fraction of crystal chains in the stretched sample is aligned. It is assumed in evaluating f_c that the crystal c-axis is cylindrically distributed around the orienting direction in the stretched sample.
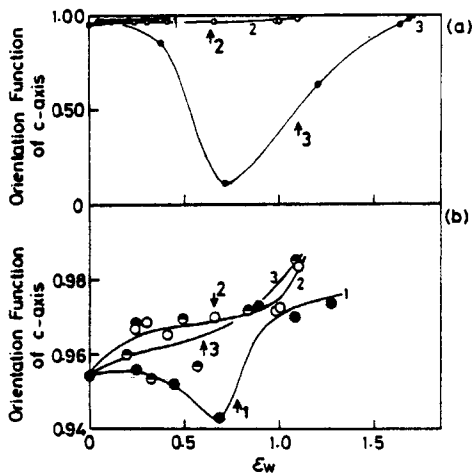

Fig. 5. Orientation function of crystal c-axis vs. ϵ_W in extension (a) $\theta = 0°$ (●), $45°$ (○), and $90°$ (◐) and $T_t = 373$ K and (b) at $\theta = 45°$ and $T_t = 313$ K (●), 373 K (○), and 403 K (◐).

The angle between this direction and the testing direction decreases with extension at $\theta = 45°$ or $90°$, but does not change at $\theta = 0°$.[6,7] Variation of the orientation function of the crystal c-axis with extension is qualitatively similar to that of the $(H_l - H_{as})/(H_l - H_{as})_0$ curve shown in Figure 4 at each testing condition.

The orientation function of amorphous chains, f_a, is evaluated by the following equation:

$$f_a = (\Delta - \chi_v f_c \Delta_c^\circ)/(1 - \chi_v) \Delta_a^\circ \qquad (7)$$

where Δ is the birefringence of the sample, χ_v the crystallinity in volume fraction, f_c the orientation function of the crystal c-axis, Δ_c° the intrinsic birefringence of crystalline region, and Δ_a° the intrinsic birefringence of amorphous region. According to Samuels,[17] the values of Δ_c° and Δ_a° in polypropylene are 0.0285 and 0.0618, respectively, and the value of form birefringence is neglected on evaluating f_a. Figures 6(a) and (b) show the variation of birefringence with extension (a) at $\theta = 0°$, $45°$, and $90°$ and $T_t = 373$ K and (b) at $\theta = 45°$ and $T_t = 313$ K, 373 K, and 403 K, respectively. The orienting direction in the stretched sample was used as principal axis in measuring birefringence. Figures 7(a) and (b) show the variation of orientation function of amorphous chains, which is evaluated by using eq. (7) and the data found in Figure 6, with extension: (a) at $\theta = 0°$, $45°$, and $90°$ and $T_t = 373$ K and (b) at $\theta = 45°$ and $T_t = 313$ K, 373 K, and 403 K, respectively. In all the testing conditions, the change of the orientation function of amorphous chains, f_a, with extension is closely similar to the change of $(H_l - H_{as})/(H_l - H_{as})_0$, as shown in Figure 4. Figure 8 shows the relationship between $(H_l - H_{as})/(H_l - H_{as})_0$ and f_a in all the testing conditions. This relationship is described as a single curve and the value of $(H_l - H_{as})/(H_l - H_{as})_0$ monotonously increased with f_a. It becomes appaent from Figure 8 that the value of $(H_l - H_{as})/(H_l - H_{as})_0$ closely depends on f_a, as presumed in the previous subsection.
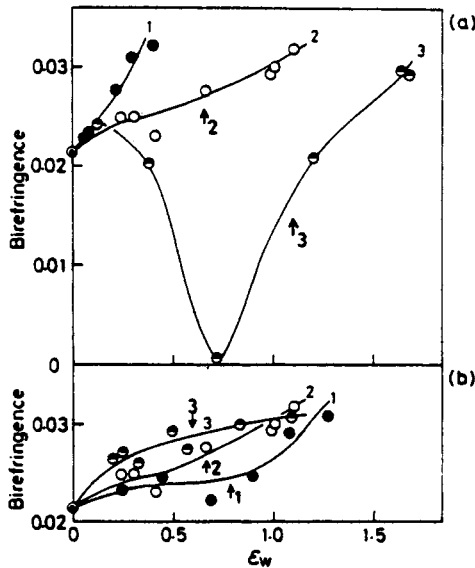

Fig. 6. Birefringence vs. ϵ_W in extension (a) at $\theta = 0°$ (●), 45° (○), and 90° (◐) and $T_t = 373$ K and (b) at $\theta = 45°$ and $T_t = 313$ K (●), 373 K (○), and 403 K (◐).
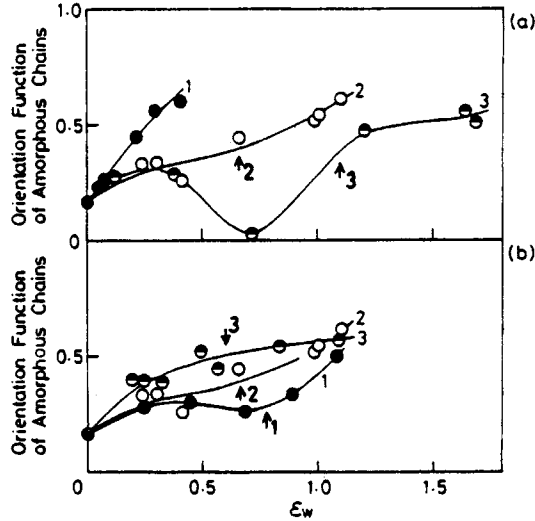
Fig. 7. Orientation function of amorphous chains vs. ϵ_W in extension (a) at $\theta = 0°$ (●), 45° (○), and 90° (◐) and $T_t = 373$ K and (b) at $\theta = 45°$ and $T_t = 313$ K (●), 373 K (○), and 403 K (◐).

The f_a increased in the later stage of extension at $\theta = 45°$ or 90° and did from the beginning of extension at $\theta = 0°$. This fact confirms the prediction in the first subsection of this section that the melting temperature is increased by the increase of f_a in the later stage of extension at $\theta = 45°$ or 90° and throughout extension at $\theta = 0°$.

Relationship Between Strain Hardening and Change of Molecular Aggregation State in Amorphous Region During Extension

Figures 9(a) and (b) show true stress–ϵ_W curves in extension (a) at $\theta = 0°, 45°$, and 90° and $T_t = 373$ K and (b) at $\theta = 45°$ and $T_t = 313$ K, 373 K, and 403 K, respectively. Since a cross-sectional area is remarkably decreased by extension, particularly at $\theta = 45°$ or 90°, it is better to use true stress instead of nominal stress. True stress σ_t is defined as follows:

$$\sigma_t = F/A$$

where F is a load at an actual cross-sectional area A at each stage of extension. From σ_t–ϵ_W curves in all the testing conditions, as shown in Figure 9, it becomes
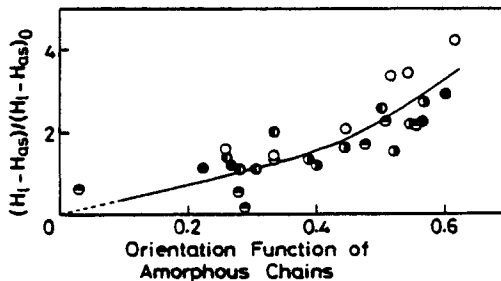

Fig. 8. $(H_l - H_{as})/(H_l - H_{as})_0$ vs. orientation function of amorphous chains in the various testing conditions: (●) 0°, 373 K; (○) 45°, 373 K; (◐) 90°, 373 K; (◑) 45°, 313 K; (◔) 45°, 403 K.
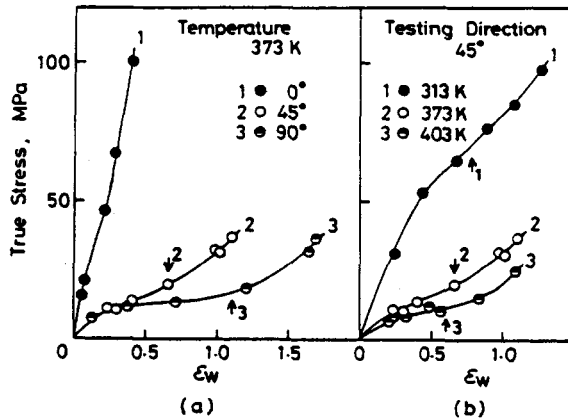
Fig. 9. True stress vs. ϵ_W in extension (a) at $\theta = 0°$ (●), 45° (○), and 90° (⊖) and $T_t = 373$ K and (b) at $\theta = 45°$ and $T_t = 313$ K (●), 373 K (○) and 403 K (⊖).

apparent that yield phenomenon is always followed by more and more increase of true stress with increasing strain, that is, strain hardening is clearly indicated. The yield point arose before the $A_2 \rightarrow \overline{A_2}$ transition indicated by the arrows in the figure took place.

Figures 10(a) and (b) show the relationships between f_A and σ_t (a) at $\theta = 0°$, 45°, and 90° and $T_t = 373$ K and (b) at $\theta = 45°$ and $T_t = 313$ K, 373 K, and 403 K, respectively. In all the testing conditions, f_a certainly increased with σ_t in the stage of higher true stress (namely, after the $A_2 \rightarrow \overline{A_2}$ transition took place at $\theta = 45°$ or 90°, as indicated by the arrows in the figure). This fact shows that the strain hardening is reflected on the increase of f_a. However, in the stage of lower true stress for $\theta = 90°$ and $T_t = 373$ K, f_a temporarily decreased with true
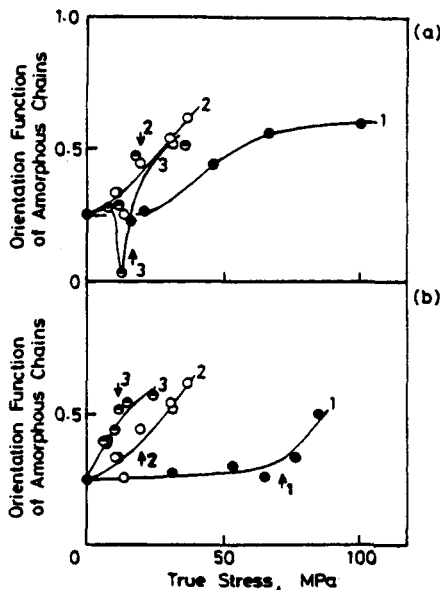

Fig. 10. Orientation function of amorphous chains. vs. true stress in extension (a) at $\theta = 0°$ (●), 45° (○), 90° (⊖) and $T_t = 373$ K and (b) at $\theta = 45°$ and $T_t = 313$ K (●), 373 K (○) and 403 K (⊖).

stress, and therefore increase of true stress was not directly reflected on the increase of f_a. The value of f_a became higher in the order of $\theta = 45°$, $\theta = 90°$, and $\theta = 0°$ under the same true stress after the $A_2 \rightarrow \overline{A_2}$ transition took place, as shown in Figure 10(a). This fact shows that increase of f_a with true stress depends on testing direction and f_a is most effectively increased in the extension at $\theta = 45°$. Stress analysis for a sample predicts that the shear stress to arbitrary plane in a sample takes the maximum value when the tensile stress is applied with an angle of 45° to the shear plane. For oriented sample, if shear deformation easily takes place along the oriented molecular axis, $\theta = 45°$ is the most preferable condition for plastic deformation.

As shown in Figure 10(b), the f_a at higher testing temperature became higher in the region of low true stress than that at lower testing temperature. The molecular mobility will be increased by increase of testing temperature and the plastic deformation can be more easily feasible to take place. However, it should be noted that the highest value of f_a was reached at the testing temperature of 373 K. Too high a testing temperature induces the increase of molecular motion and rather disturbs to achieve high f_a value.

CONCLUSION

The preoriented isotactic polypropylene was uniaxially stretched under five testing conditions, that is, at $\theta = 0°$ and $T_t = 373$ K, at $\theta = 45°$ and $T_t = 313$ K, at $\theta = 45°$ and $T_t = 373$ K, at $\theta = 45°$ and $T_t = 403$ K, and at $\theta = 90°$ and $T_t = 373$ K. The following conclusions are drawn out:

(1) At $\theta = 45°$ or $90°$, the melting temperature decreased in the earlier stage of extension (namely, before the $A_2 \rightarrow \overline{A_2}$ transition takes place). This decrease is caused by the decrease of crystallite thickness, which was observed due to the uniform shear deformation. In the later stage of extension (namely, after the $A_2 \rightarrow \overline{A_2}$ transition takes place), the melting temperature was not only affected by the crystallite thickness but by the orientation function of amorphous chains, f_a. The melting behavior at $\theta = 0°$ corresponded to that in the later stage of extension at $\theta = 45°$ or $90°$, from the beginning of drawing.

(2) The ratio $(H_l - H_{as})/(H_l - H_{as})_0$ of the "melting" enthalpy of the amorphous region after extension to that before extension monotonously increased with f_a. The value of $(H_l - H_{as})/(H_l - H_{as})_0$ is uniquely determined by f_a, independent of both testing direction and testing temperature.

(3) The strain hardening was reflected on the observation that f_a increased in the later stage of extension at $\theta = 45°$ or $90°$ and in the whole process of extension at $\theta = 0°$. The value of f_a most effectively increased in the extension at $\theta = 45°$ and the highest value of f_a was reached at the testing temperature of 373 K.

References

1. G. Meinel and A. Peterlin, *J. Polym. Sci.*, A-2, **9**, 67 (1971).
2. R. G. C. Arridge and P. J. Barham, *J. Polym. Sci., Polym. Phys. Ed.*, **16**, 1297 (1978).
3. A. Peterlin and G. Meinel, *J. Appl. Phys.*, **36**, 3028 (1965).
4. W. G. Harland, M. M. Khadr, and P. H. Peters, *Polymer*, **15**, 81 (1974).
5. R. J. Samuels, *J. Polym. Sci., Polym. Phys. Ed.*, **13**, 1417 (1975).
6. K. Yamada and M. Takayanagi, *Kobunshi Ronbunshu*, **34**, 465 (1977).
7. K. Yamada and M. Takayanagi, *J. Appl. Polym. Sci.*, **24**, 781 (1979).

8. Z. W. Wilchinsky, *J. Appl. Polym. Sci.*, **7**, 923 (1963).

9. J. D. Hoffman and J. J. Weeks, *J. Res. Natl. Bur. Std.*, **66A**, 13 (1962).

10. N. Hirai and S. Yamashita, *Kobunshi-Kagaku*, **21**, 173 (1964).

11. J. G. Fatou, *Eur. Polym. J.*, **7**, 1057 (1971).

12. J. G. Fatou and L. Mandelkern, *J. Phys. Chem.*, **69**, 417 (1965).

13. H. E. Bair, R. Salovey, and T. W. Huseby, *Polymer*, **8**, 9 (1967).

14. F. Danusso, G. Moraglio, and G. Natta, *Ind. Plast. Mod.*, **10**, 40 (1958).

15. M. Iguchi, *Makromol. Chem.*, **177**, 549 (1976).

16. T. Hatakeyama, *Seni-Gakkai-Shi*, **31**, 289 (1975).

17. R. J. Samuels, *J. Polym. Sci. C*, **20**, 253 (1967).